

Adiabatic and nonadiabatic static polarizabilities of H and H₂

Juha Tiihonen,^{*} Ilkka Kylänpää, and Tapio T. Rantala

Department of Physics, Tampere University of Technology, P.O. Box 692, FI-33101 Tampere, Finland

(Received 24 March 2015; published 12 June 2015)

The path-integral Monte Carlo method is employed to evaluate static (hyper)polarizabilities of small hydrogen systems at finite temperature. Exact quantum statistics are obtained for hydrogen atom and hydrogen molecule immersed in homogeneous electric field. The method proves to be reliable and yields perfect agreement with known values of static polarizabilities in both adiabatic and nonadiabatic simulations. That is, we demonstrate how electronic, rotational, and vibrational contributions can be evaluated either separately or simultaneously. Indeed, at finite temperature and nonzero-field strengths we observe considerable rovibrational effects in the polarization of the hydrogen molecule. Given sufficient computational resources, the path-integral Monte Carlo method turns out to be a straightforward tool for describing and computing static polarizabilities for traditionally challenging regimes.

DOI: [10.1103/PhysRevA.91.062503](https://doi.org/10.1103/PhysRevA.91.062503)

PACS number(s): 31.15.A–, 32.10.Dk, 33.15.Kr

I. INTRODUCTION

Polarizability is a fundamental property of matter, describing its response to the external electric fields. It has straightforward manifestations in linear and nonlinear optical phenomena and thus it has a significant role in the interpretation of experimental data and development of new technology [1]. Current *ab initio* methods for quantum scale modeling of polarizability result from many decades of development. Nevertheless, while these provide high accuracy at 0 K, their applicability is limited in many central real-world aspects such as high temperatures, finite particle densities, and rovibrational effects. Here we propose a different approach, which could overcome these problems in a straightforward manner for the benefit of, e.g., cold-atom physics [1], astrophysics [2], and spectroscopy [3] and thus make important bridges from *ab initio* to the practical world.

The polarizability is conventionally divided into components as a perturbation expansion. For example, in the Buckingham convention [4] the total energy of a system in a constant electric field (Stark effect) is expressed as

$$E^{(1)} = E^{(0)} - \mu_{\alpha}^{(0)} F_{\alpha} - \frac{1}{2} \alpha_{\alpha\beta} F_{\alpha} F_{\beta} - \frac{1}{6} \beta_{\alpha\beta\gamma} F_{\alpha} F_{\beta} F_{\gamma} - \frac{1}{24} \gamma_{\alpha\beta\gamma\delta} F_{\alpha} F_{\beta} F_{\gamma} F_{\delta} - \dots \quad (1)$$

with permanent dipole moment $\mu_{\alpha}^{(0)}$, static dipole polarizability $\alpha_{\alpha\beta}$, and first and second hyperpolarizabilities $\beta_{\alpha\beta\gamma}$ and $\gamma_{\alpha\beta\gamma\delta}$, respectively. In addition, the expression for the induced dipole moment reduces to

$$\begin{aligned} \mu_{\alpha}^{(1)} &= - \frac{\partial E^{(1)}}{\partial F_{\alpha}} \\ &= \mu_{\alpha}^{(0)} + \alpha_{\alpha\beta} F_{\beta} + \frac{1}{2} \beta_{\alpha\beta\gamma} F_{\beta} F_{\gamma} + \frac{1}{6} \gamma_{\alpha\beta\gamma\delta} F_{\beta} F_{\gamma} F_{\delta} + \dots, \end{aligned} \quad (2)$$

where indices $\alpha, \beta, \gamma, \delta, \dots$ refer to Einstein summation of distinct tensor components.

The polarizabilities are usually calculated with either sum-over-states [5] or finite-field (FF) approaches [6]. Sum-over-states formulas are exact, but they become extensively complicated for higher-rank polarizabilities. Also, their computation

typically involves limited basis sets. The FF principle is based on calculating the perturbations in multiple finite-field strengths and then extrapolating the differentials to zero field [7], e.g.,

$$\alpha_{\alpha\beta} = \left. \frac{\partial^2 E^{(1)}}{\partial F_{\alpha} \partial F_{\beta}} \right|_{F=0}. \quad (3)$$

This can be done with a variety of methods. Basically, the challenge is to approximate solutions to the system, which is fundamentally unstable in any nonzero constant electric field.

Moreover, electron-nucleus coupling and internuclear motion have to be treated in order to obtain total polarizabilities. This is commonly performed with the so-called clamped-nucleus approximation, i.e., supplementing electronic polarizability with rotational and vibrational components [8]:

$$\alpha^{\text{tot}} = \alpha^{\text{el}} + \alpha^{\text{rot}} + \alpha^{\text{vib}}, \quad (4)$$

where α^{tot} is the total polarizability. This cumbersome separation can be overcome with a nonadiabatic Hylleraas basis approach, which, however, is limited to three particles only [9].

Overall, the extent of the finite-field response is built upon increasingly complicated series of properties. This combined with finite-temperature statistics makes consideration of electric-field phenomena a formidable task with conventional methods. In this work we introduce a more holistic approach: the path-integral Monte Carlo (PIMC) approach [10–13] applied in the study of electric-field phenomena and calculation of polarizabilities. We were able to find only a couple of studies [14,15] vaguely geared in this direction.

Thus, we present a comprehensive and accurate study of static polarizabilities of neutral hydrogen atoms and molecules. These two- and four-particle systems are considered both adiabatically and nonadiabatically, i.e., with and without the Born-Oppenheimer (BO) approximation. Also, it should be emphasized that with the PIMC approach all the terms in Eqs. (1) and (2) are implicitly included. We will demonstrate that the nonrelativistic PIMC approach is a straightforward and efficient tool for studying electric-field effects including the inherent temperature dependence.

^{*}Corresponding author: juha.tiihonen@tut.fi

II. METHOD

For interacting distinguishable particles the Feynman formulation of quantum-statistical mechanics [16] gives the partition function as a trace of the density matrix

$$Z = \text{Tr} \hat{\rho}(\beta) = \int dR_0 dR_1 \cdots dR_{M-1} \prod_{i=0}^{M-1} e^{-S(R_i, R_{i+1}; \tau)},$$

where $\hat{\rho}(\beta) = e^{-\beta \hat{H}}$, S is the action, $\beta = 1/k_B T$, $\tau = \beta/M$, $R_M = R_0$, and M is called the Trotter number. We use the pair approximation in the action [10,17] for the Coulomb interaction of charges. For neutral systems the external potential arising from the homogeneous finite electric field yields an additional diagonal term in the action, i.e., [18]

$$U_{\text{ext}}(R; \tau) = -\tau \mu_\alpha F_\alpha = -\tau F_\alpha q_n r_{n\alpha}, \quad (5)$$

where R is the configuration at given time slice, F_α is the electric field, and q_n is the charge of the n th particle, where n denotes summation over all particles. Sampling in the configuration space is carried out using the Metropolis procedure [19] with multilevel bisection moves [20]. We use both the thermal estimator [10] and the virial estimator [21] in the calculation of total energy.

In our model all the particles are described as boltzmannons, i.e., they obey the Boltzmann statistics. Since we are dealing with the hydrogen atom and the ground state of the H_2 molecule the particles involved can accurately be treated as distinguishable particles. In the case of the hydrogen molecule this is possible in the singlet state by assigning spin up to one electron and spin down to the other one and applying the same for the positive particles. This is accurate enough, as long as the thermal energy is well below that of the lowest electronic triplet excitation. At $T \approx 160$ K this is the case for the hydrogen molecule [11]. This fact can also be exploited in the calculations of BO energetics at the equilibrium internuclear distance. Therefore, within our BO simulations we may use temperatures up to a few thousand Kelvin and still the system remains in its electronic ground state (see, for example, the BO results in Fig. 1 of Ref. [12]). The numerical gain is a smaller statistical error in less time.

It should be emphasized that for systems consisting of distinguishable particles the accuracy of the PIMC method is determined only by the imaginary-time time step τ . As τ approaches zero the exact many-body results are obtained within the numerical precision.

We use atomic units in this work and thus the lengths, energies, and masses are given in units of the Bohr radius a_0 , hartree E_h , and free-electron mass m_e , respectively. Therefore, we have $m_e = 1$ as the mass of the electrons and for the protons we use $m_p = 1836.152\,672\,48 m_e$. We use the imaginary-time time step $\tau = \beta/M = 0.03 E_h^{-1}$, which ensures very good accuracy [13]. Our Trotter number $M = 2^{16}$ together with the time step τ result in a 160.6 K simulation temperature. For the BO calculations we use higher temperature for better statistics, but as discussed above we are still sampling the correct electronic state. The statistical standard error of the mean with 2σ limits is used as an error estimate for the observables. The simulations are carried out in a periodic cubic simulation cell $V = (150a_0)^3$, where we apply the minimum image convention.

III. RESULTS

We present PIMC results for the hydrogen atom H and hydrogen molecule H_2 both adiabatically and nonadiabatically. The adiabatic calculations are carried out with fixed nuclei and will be referred as electronic BO calculations. The nonadiabatic calculations with freely moving quantum nuclei include full account of electron-nuclei coupling and are called all quantum (AQ). In general, we are able to separate electronic, rotational, and vibrational contributions by restricting motion of the chosen degrees of freedom.

We have chosen a few finite-field strengths F_z ($E_h e^{-1} a_0^{-1}$), in which we compute the induced perturbations in dipole moment and total energy. We confirm that a reasonably weak strength of the field ensures a *metastable* equilibrium state, where quantum statistics can be sampled without risk of dissociation, i.e., electrons tunneling apart from the nuclei due to the electric field.

The results are compared with finite-field reference models constructed from Eqs. (1) and (2) (as in Ref. [7]) and known values for polarizabilities from the literature [22–26]. For atoms and molecules with a zero permanent dipole moment, i.e., $\mu^{(0)} = 0$, also $\beta_{zzz} = 0$ [8]. It should be emphasized that the reference model is for 0 K temperature, it is only exact at the zero-field limit, and while considered only up to γ_{zzzz} , it is subject to a truncation error.

We begin with computation of the H atom. The only difference between the BO and AQ cases is in the ground-state

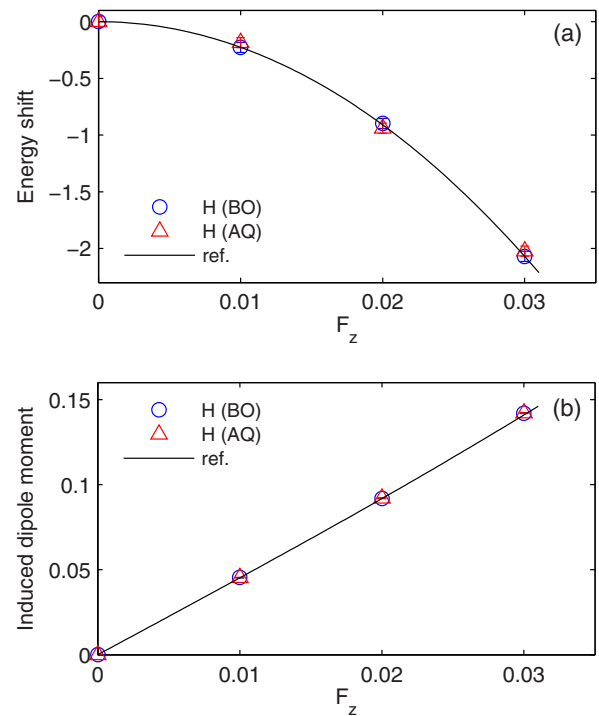


FIG. 1. (Color online) (a) Stark shift (in mhartree) and (b) induced dipole moment (ea_0) of the hydrogen atom as functions of the external electric field. The energy shift is the difference between perturbed and unperturbed total energies $\Delta E^{(1)} = E^{(1)} - E^{(0)}$. Blue circles represent BO results, red triangles represent AQ results, and the solid line is the reference model (see Table I).

TABLE I. Energy shift $\Delta E^{(1)} = E^{(1)} - E^{(0)}$ (in mhartree) and induced dipole moment (ea_0) of the H atom, also visualized in Fig. 1. The column labeled “Difference” represents the difference between values from the closest available reference model [22,23] and the PIMC results.

Calculation	F_z	$\Delta E^{(1)}$	ΔE^{ref}	Difference	$\Delta\mu^{(1)} \times 10^2$	$\Delta\mu^{\text{ref}} \times 10^2$	Difference
BO	0.0	0.000(52)	0.0	0.000(52)	0.004(15)	0.0	-0.004(15)
	0.01	-0.227(39)	-0.2256	0.002(39)	4.530(12)	4.5222	-0.008(12)
	0.02	-0.898(39)	-0.9089	-0.011(39)	9.197(14)	9.1778	-0.019(14)
	0.03	-2.069(39)	-2.0700	-0.001(39)	14.203(16)	14.099	-0.103(16)
AQ	0.0	0.000(50)		0.000(50)	-0.008(17)		0.008(17)
	0.01	-0.185(45)		-0.040(45)	4.536(13)		-0.013(13)
	0.02	-0.939(45)		0.030(45)	9.195(15)		-0.018(15)
	0.03	-2.023(45)		-0.047(45)	14.208(18)		-0.109(18)

energy: With a virial estimator we get (in zero field) $E^{(0)}(\text{BO}) = -0.499\,97(5)$ and $E^{(0)}(\text{AQ}) = -0.499\,71(5)$ against exact $E^{\text{ref}}(\text{BO}) = -0.5$ and $E^{\text{ref}}(\text{AQ}) = -0.499\,727\,8$, respectively. In Fig. 1(a) we present the energy shift and in Fig. 1(b) we give the induced dipole moment for a few finite-field values. We employ the same BO reference model to both cases and they both yield excellent agreement. However, in stronger fields, e.g., $F_z = 0.03$, the truncation error, i.e., exclusion of the fourth hyperpolarizability $\epsilon_{zzzzz} = 3.533\,595 \times 10^6$ [23], is large enough to be observed as a small difference between our result and the reference. These results are also given numerically in Table I.

The static (hyper)polarizabilities are obtained by nonlinear regression on our results. We use the data for the induced dipole moment because its estimator is statistically more precise compared to those of the total energy. The fitted polarizabilities for hydrogen are shown in Table II. Our static dipole polarizabilities α are accurate within 95% confidence estimates and second hyperpolarizabilities γ are slightly overestimated due to truncation error. Generally, the static dipole polarizabilities have much smaller error than the second hyperpolarizabilities.

The adiabatic simulations of the H_2 molecule are performed at the equilibrium distance $R_e = 1.40a_0$ [24] and, unlike other calculations, using a thermal estimator for the total energy [10]. To compensate for the high variance of the thermal estimator, we boost the efficiency by computing at higher temperature $T = 2500$ K, which, as argued earlier, is still close enough to the low-temperature clamped-nuclei density matrix. Our

TABLE II. Static dipole polarizabilities and second hyperpolarizabilities of H with 95% confidence intervals are obtained using nonlinear regression on our PIMC results. They are compared to the 0 K references found in the literature.

	α_{zz} (BO)	$\bar{\alpha}$ (AQ)
H	4.496(23) ^a	4.496(39) ^a
	4.500 ^b	
	γ_{zzzz} (BO)	$\bar{\gamma}$ (AQ)
	1586(184) ^a	1592(316) ^a
	1333.125 ^c	

^aThis work (160 K).

^bReference [22].

^cReference [23].

ground-state energy without the external field is $E^{(0)}(\text{BO}) = -1.174\,34(18)$, which is close to the highly accurate quantum chemistry estimate of $E^{\text{ref}}(\text{BO}) = -1.174\,474\,77$ [25]. The adiabatic hydrogen molecule is considered in the two extreme orientations in laboratory coordinates: perpendicular \perp or parallel \parallel to the external field. Computation of intermediate orientation angles could be done just as easily, but it is not considered here. Changes in total energy and induced dipole moment are presented in Figs. 2(a) and 2(b), respectively, and corresponding numerical values are given in Table III. These results demonstrate good agreement in both orientations. Using the procedure similar to that for the H atom, we obtain

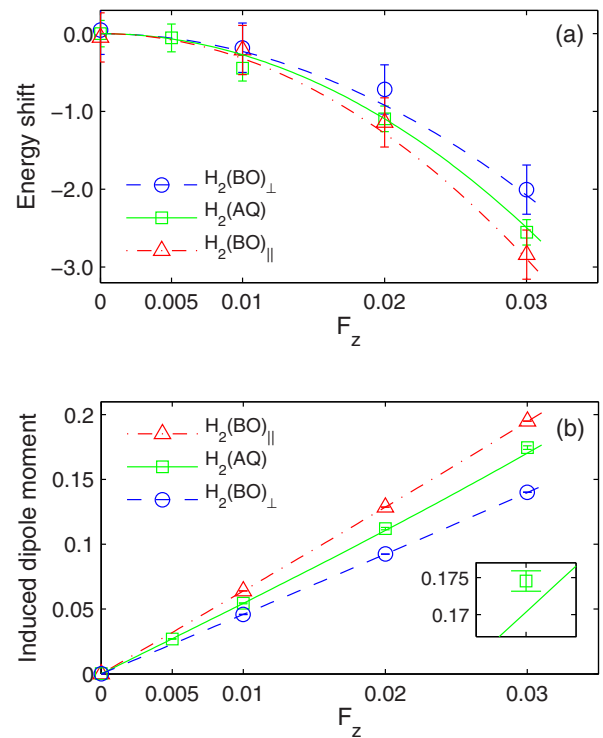


FIG. 2. (Color online) (a) Stark shift (in mhartree) and (b) induced dipole moment (ea_0) of the hydrogen molecule as functions of the external electric field. The energy shift is the difference between perturbed and unperturbed total energies $\Delta E^{(1)} = E^{(1)} - E^{(0)}$. Blue circles represent BO (\perp) results, red triangle represent BO (\parallel) results, green squares represent AQ results, and lines are the corresponding reference models (see Table III).

TABLE III. Energy shift $\Delta E^{(1)} = E^{(1)} - E^{(0)}$ (in mhartree) and induced dipole moment (ea_0) of the H_2 molecule, also visualized in Fig. 2. The column labeled “Difference” represents the difference between values from the closest available reference model [24–26] and the PIMC results.

Calculation	F_z	$\Delta E^{(1)}$	ΔE^{ref}	Difference	$\mu_z^{(1)} \times 10^2$	$\mu_z^{\text{ref}} \times 10^2$	Difference
BO $_{\parallel}$	0.0	-0.048(317)	0.0	0.048(317)	-0.003(11)	0.0	0.003(11)
	0.01	-0.211(316)	-0.3196	-0.109(316)	6.399(11)	6.3984	-0.001(11)
	0.02	-1.141(316)	-1.2820	-0.141(316)	12.867(11)	12.865	-0.002(11)
	0.03	-2.841(316)	-2.8972	-0.057(316)	19.468(11)	19.468	-0.034(11)
BO $_{\perp}$	0.0	0.048(317)	0.0	-0.048(317)	0.002(11)	0.0	-0.002(11)
	0.01	-0.181(317)	-0.2292	-0.048(317)	4.590(11)	4.5886	-0.002(11)
	0.02	-0.717(317)	-0.9196	-0.202(317)	9.236(11)	9.2348	-0.001(11)
	0.03	-2.006(317)	-2.0800	-0.074(317)	13.996(11)	13.996	-0.022(11)
AQ	0.0	0.000(170)		0.000(170)	0.019(48)		-0.019(48)
160 K	0.005	-0.054(179)		-0.013(179)	2.699(28)		-0.012(28)
	0.01	-0.443(165)		0.172(165)	5.453(41)		-0.010(41)
	0.02	-1.095(166)		0.000(166)	11.205(91)		-0.143(91)
	0.03	-2.554(163)		0.058(163)	17.453(138)		-0.419(138)
AQ	0	0.000(296)	0.0	0.000(296)	0.037(47)	0.0	-0.037(47)
295 K	0.005	-0.082(322)	-0.0677	0.014(322)	2.738(53)	2.7106	-0.028(53)
	0.01	-0.494(250)	-0.2714	0.222(250)	5.443(51)	5.4433	0.001(51)
	0.02	-1.316(253)	-1.0945	0.222(253)	11.063(81)	11.063	-0.052(81)
	0.03	-2.686(247)	-2.4958	0.190(247)	17.148(131)	17.035	-0.113(131)

static dipole polarizabilities and second hyperpolarizabilities, which are shown in Table IV. The error bars can be made smaller by additional computational labor.

Nonadiabatic calculations of H_2 include rovibrational effects arising from the chosen finite temperature and influenced by the external electric field. It should be pointed out that with the nonadiabatic PIMC approach the electron-nuclei coupling is exactly included and thus in our simulations we sample an accurate many-body density matrix at finite temperature and in an external electric field. For the nonadiabatic molecule the equilibrium distance is slightly larger compared to the case of static nuclei and this is also accurately taken into account [11]. To compare ground-state energies, we extrapolate our finite-temperature energy to 0 K, which yields $E_{0\text{K(AQ)}}^{(0)} = -1.16387(18)$, which coincides with the 0 K reference

TABLE IV. Static dipole polarizabilities and second hyperpolarizabilities of H_2 with 95% confidence intervals are obtained using nonlinear regression on 160 K PIMC results. They are compared to the 0 K references found in the literature.

	$\alpha_{zz}(\text{BO})_{\parallel}$	$\alpha_{xx}(\text{BO})_{\perp}$	$\bar{\alpha}(\text{AQ})$
H_2	6.382(13) ^a	4.577(10) ^a	5.417(37) ^a
	6.387493 ^c	4.57861 ^c	5.4139 ^d
			5.428(59) ^b
	$\gamma_{zzzz}(\text{BO})_{\parallel}$	$\gamma_{xxxx}(\text{BO})_{\perp}$	$\bar{\gamma}(\text{AQ})$
	787(100) ^a	640(73) ^a	2678(298) ^a
	682.5 ^c	575.9 ^c	1763 ^e
			1918(479) ^b

^aThis work (160 K).

^bThis work (295 K).

^cReference [24].

^dReference [25].

^eReference [26] (295 K).

value $E^{\text{ref}}(\text{AQ}) = -1.1640250185$ [27]. Our simulations at $T = 160.6$ K demonstrate good agreement in the shift of the total energies, in the induced dipole moment, and in the fitted polarizabilities (see Fig. 2 and Tables IV and III).

It is important to understand that the exact polarizabilities in finite-temperature equilibrium obey the Maxwell-Boltzmann distribution of excited-state contributions. With the adiabatic and the monatomic cases, these reduce to electronic ground states at low temperatures, but this is not the case with $H_2(\text{AQ})$, whose excited rotational states are considerably occupied at $T = 160.6$ K. By thermal averaging [8] it can be shown that the total hyperpolarizability may vary significantly with temperature. This can be seen from Fig. 2 and Table III, where the induced dipole moment of $H_2(\text{AQ})$ has a slightly higher value at 160.6 K (PIMC approach) than at the 295 K reference [26]. Indeed, comparison of the obtained hyperpolarizabilities in Table IV shows that $\bar{\gamma}(160.6\text{ K}) =$

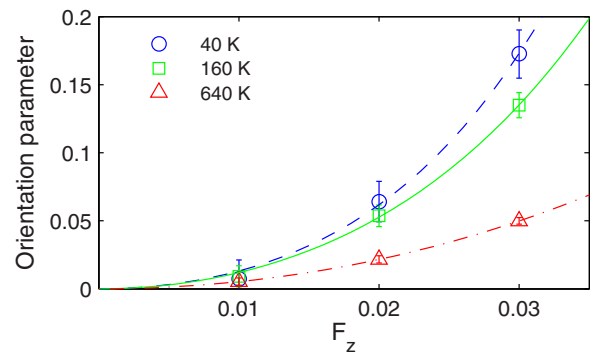


FIG. 3. (Color online) Orientation parameter of H_2 plotted against the external field strength at different temperatures. Blue circles represent 40 K, green squares 160 K, and red triangles 640 K results. Solid lines are quadratic fits to guide the eye.

TABLE V. Orientation parameter of the hydrogen molecule H_2 as a function of T (visualized in Fig. 3).

	T (K)	F_z		
		0.01	0.02	0.03
H_2	40	0.007(14)	0.064(15)	0.173(18)
	160	0.009(8)	0.054(8)	0.135(9)
	640	0.005(3)	0.021(3)	0.050(3)

2678(298) is considerably higher than $\bar{\gamma}(295 \text{ K}) = 1918(479)$ or the reference value $\bar{\gamma}^{\text{ref}}(295 \text{ K}) = 1763$ [26], which is estimated according to Eq. (4). Static dipole polarizability $\bar{\alpha}$ is predicted to increase slightly with the temperature [25], however, the effect is lost here within error boundaries.

The rotational coupling with the electric field can be further examined by the orientation parameter

$$S = \frac{1}{2}(3 \cos^2 \theta - 1), \quad (6)$$

where θ is the angle between the laboratory axis (electric field) and that of the diatomic H_2 . The perpendicular configuration gives the lower limit $S = -\frac{1}{2}$ and the parallel configuration the upper limit $S = 1$; random orientation gives the expectation value of $\langle S \rangle = 0$. The parameter is computed for $H_2(\text{AQ})$ in different field strengths and temperatures using lower accuracy ($\tau \approx 1$) for feasible efficiency. Our results are presented in Fig. 3 and in Table V. While the static total polarizability peaks at parallel orientation, the estimate of S increases towards 1 in stronger fields and more so at lower temperatures, where thermal distortion is smaller.

IV. CONCLUSION

In this work we presented a path-integral Monte Carlo study of the hydrogen atom and hydrogen molecule in a weak homogeneous static electric field. We demonstrated accurate finite-field results for the Stark shift and induced dipole moment, which agree excellently with the Buckingham perturbation expansion, i.e., Eqs. (1) and (2) in the low-temperature regime. Also, our extrapolated values for static (hyper)polarizabilities match within confidence bounds the most accurate ones found in the literature.

We showed that with path integrals it is straightforward to extend the conventional analysis by taking into account the nonadiabatic effects and those from finite temperature. This also supports the extensive work by Bishop on finite-temperature effects on polarizabilities [8]. To this end, we also demonstrated how the orientation of the hydrogen molecule behaves as a function of the electric-field strength. While we do not yet report any nonequilibrium statistics or comprehensive finite-temperature dependences, it is evident that this approach permits access to *ab initio* study of unexplored electric-field phenomena.

ACKNOWLEDGMENTS

We acknowledge CSC-IT Center for Science Ltd. and Tampere Center for Scientific Computing for the allocation of computational resources. We gratefully acknowledge support from the Academy of Finland.

-
- [1] J. Mitroy, M. S. Safronova, and C. W. Clark, *J. Phys. B* **43**, 202001 (2010).
- [2] G. J. Harris, A. E. Lynas-Gray, S. Miller, and J. Tennyson, *Astrophys. J.* **600**, 1025 (2004).
- [3] N. Subramanian, A. F. Goncharov, M. Somayazulu, and R. J. Hemley, *J. Phys.: Conf. Ser.* **215**, 012057 (2010).
- [4] A. D. Buckingham, *Advances in Chemical Physics* (Wiley, New York, 2007), pp. 107–142.
- [5] D. P. Shelton and J. E. Rice, *Chem. Rev.* **94**, 3 (1994).
- [6] H. D. Cohen and C. C. J. Roothaan, *J. Chem. Phys.* **43**, S34 (1965).
- [7] J. Kobus, *Phys. Rev. A* **91**, 022501 (2015).
- [8] D. M. Bishop, *Rev. Mod. Phys.* **62**, 343 (1990).
- [9] L.-Y. Tang, Z.-C. Yan, T.-Y. Shi, and J. F. Babb, *Phys. Rev. A* **90**, 012524 (2014).
- [10] D. M. Ceperley, *Rev. Mod. Phys.* **67**, 279 (1995).
- [11] I. Kylänpää, T. T. Rantala, and D. M. Ceperley, *Phys. Rev. A* **86**, 052506 (2012).
- [12] I. Kylänpää and T. T. Rantala, *J. Chem. Phys.* **133**, 044312 (2010).
- [13] I. Kylänpää and T. T. Rantala, *J. Chem. Phys.* **135**, 104310 (2011).
- [14] D. Shin, M.-C. Ho, and J. Shumway, [arXiv:quant-ph/0611105](https://arxiv.org/abs/quant-ph/0611105).
- [15] H. Nagao, K. Ohta, M. Nakano, and K. Yamaguchi, *Int. J. Quantum Chem.* **65**, 697 (1997).
- [16] R. P. Feynman, *Statistical Mechanics* (Perseus, Reading, 1998).
- [17] R. G. Storer, *J. Math. Phys.* **9**, 964 (1968).
- [18] J. Tiihonen, Master's thesis, Tampere University of Technology, 2014.
- [19] N. Metropolis, A. W. Rosenbluth, M. N. Rosenbluth, A. H. Teller, and E. Teller, *J. Chem. Phys.* **21**, 1087 (1953).
- [20] C. Chakravarty, M. C. Gordillo, and D. M. Ceperley, *J. Chem. Phys.* **109**, 2123 (1998).
- [21] M. F. Herman, E. J. Bruskin, and B. J. Berne, *J. Chem. Phys.* **76**, 5150 (1982).
- [22] I. Waller, *Z. Phys.* **38**, 635 (1926).
- [23] G. L. Sewell, *Math. Proc. Camb. Philos. Soc.* **45**, 631 (1949).
- [24] D. M. Bishop, J. Pipin, and S. M. Cybulski, *Phys. Rev. A* **43**, 4845 (1991).
- [25] W. Kolos and L. Wolniewicz, *J. Chem. Phys.* **49**, 404 (1968).
- [26] D. M. Bishop and B. Lam, *Chem. Phys. Lett.* **143**, 515 (1988).
- [27] M. Stanke, D. Kędziera, S. Bubin, M. Molski, and L. Adamowicz, *J. Chem. Phys.* **128**, 114313 (2008).